Thermal Analysis of Casson Hybrid Nanofluid Flow over a Riga Plate in Porous Media with QuadraticThermal Radiation

Ephesus O. Fatunmbi,[1] Sulyman O. Salawu[2]
[1]Department of Mathematics and Statistics, Federal Polytechnic, Ilaro, Nigeria.
[2]Department of Mathematics, Bowen University, Nigeria.
Corresponding Email: ephesus.fatunmbi@federalpolyilaro.edu.ng

Abstract
The enhanced heat transfer characteristics of hybridized nanofluids—particularly in energy, aerospace, and electronic cooling applications, have established them as promising coolants in modern thermal management systems. Thus, this study presents a thermal analysis of water-based Casson hybrid nanofluid flow across a Riga plate embedded in a porous medium, with consideration of quadratic thermal radiation. The hybrid nanofluid comprises silicon dioxide (SiO_2) and molybdenum disulfide (MoS_2) nanoparticles suspended in a Casson fluid base, forming a non-Newtonian medium with yield stress behaviour. The Darcy–Brinkman model is employed to simulate both flow resistance in the porous matrix and electromagnetic actuation from the Riga plate. By applying similarity transformations, the governing partial differential equations are reduced to a system of nonlinear ordinary differential equations, which are then solved numerically. The findings which are presented in graphical forms offer insights into enhancing thermal performance in porous structures and optimizing advanced cooling technologies. The results reveal that increasing nanoparticle concentration and radiation intensity significantly enhance thermal conductivity and surface heat transfer. These findings support the development of high-efficiency thermal systems and advanced cooling technologies for porous media applications.
Keywords: Casson fluid; Hybrid nanofluid; Quadratic thermal radiation; Riga Plate; Porous medium

1. Introduction

Nanotechnology bridges science and engineering through the design and application of materials at the nanometer scale. Nanoparticles within the 1–100 nm range exhibit unique properties due to high surface area-to-volume ratios and quantum effects. When dispersed in base fluids, these particles form nanofluids, which significantly enhance thermal conductivity, viscosity, and heat transfer performance. Nanofluids have found applications in energy, biomedical, and industrial systems, [1-3]. In its initial conceptualization, Choi and Eastman [4] reported improved thermal conductivity, while Buongiorno [5] studied convective transport mechanisms of nanofluids. Fatunmbi et al. [6] evaluated such a phenomenon on MHd micropolar fluid consisting tiny nanoparticles. The fluid flow is configured in 2D extending vertical plate experiencing isothermal and convective wall conditions. Salawu et al. [7] incorporated the effects of nonlinear radiative heat flux to discuss MHD heat and mass transfer of Maxwell fluid containing nanoparticles over a porous medium with chemical reaction Ferdows et al. [8] and Xiu et al. [9] analyzed nanofluid behaviour in nonlinear and radiative conditions. The growing need for efficient heat transfer technologies has driven interest in hybrid nanofluids, which combine multiple nanoparticles to enhance flow and thermal properties.

Hybrid nanofluids which are formed by suspending two or more types of nanoparticles in a base fluid synergize the advantages of individual constituents to achieve enhanced thermophysical properties. Suneetha et al. [10] reported a detail review of hybrid nanofluid. The repot emphasized that hybridized nanofluid possess higher thermal conductivity which in turn offer better heat transfer capability than the single nanofluid and the regular fluids. Common nanoparticle types include metals (Au, Ag, Cu), metal oxides (TiO_2, SiO_2, Al_2O_3, MoS_2), and carbon-based materials (CNTs, graphene). Several researchers have explored hybrid combinations such as Ag–TiO, Fe_3O_4–$CoFe_2O$, Cu–Al_2O, Ag–MoS_2, SWCNT–MWCNT [11], and MoS_2-SiO_2 [12]. Among these, MoS_2–SiO_2 in a water base has gained particular interest due to its favorable mechanical, thermal, and stability characteristics, ideal for high-efficiency thermal systems. Fatunmbi et al. [13] investigated the mechanism of hybridized nanofluid formed by the mixture of copper and aluminum oxide nanoparticles with water as a base fluid. The authors incorporated the impact of thermal radiation, Ohmic and viscous heating in the model and solved the model equation

numerically. Salawu et al [14] explored thermal efficiency of hybrid nanofluid using the mixture of TiO_2, and MgO nanoparticles in Prandtl-Eyring water-based solvent.
Fatunmbi et al. [15] investigated thermal melting performance of MHD hybrid nanoliquid passing through a stretchy surface with variable thickness.

To augment heat transfer capabilities of hybrid nanoparticles, a water-based fluid with Casson like properties can be considered. The rheological behaviour of Casson fluid allows flexibility usages as required in flow control, such as industrial or biomedical processes. The yield stress provides sedimentation of nanoparticles stability, the particles combination allows optimization for particular rheological and thermal properties. Fatunmbi and Okoya 16] discussed the dynamics of heat transfer of Casson nanofluid passing a nonlinear a nonlinear extending plate towards a stagnation point. The authors examined the influence of porous medium, thermophoresis, and variable thermal conductivity. Salawu et al. [17]. considered such a non-Newtonian fluid with efficient thermal performance in the presence of composite nanomaterials, Other relevant reports on hybrid nanofluid can be found in Refs [17-19]. A Riga plate is a device known as electromagnetic actuator which induces a Lorentz force parallel to its own surface, and useful in fluid flow dynamics. It is made up of a spanwise array of irregular electrodes and perpetual magnets fixed on a horizontal plate, generating a force that that declines in an exponential form from the surface. This configuration allows for precise control over boundary layer behaviour, making it valuable in applications such as drag reduction, heat transfer enhancement, and flow stabilization. The related reports on Riga plate can be found in Refs [20-23], However, none of these studies investigated the influence of a quadratic thermal radiation on the flow dynamics of a hybridized Casson fluid. Thus, the present study aims to fill this gap in the literature.
The intent of the current study is to employ the Casson fluid model to capture the non-Newtonian behaviour of a hybrid nanofluid, providing valuable insights into its rheological properties. The focus is on investigating the thermal behaviour of a water-based hybridized nanofluid with quadratic thermal radiation using MoS_2 and SiO_2 nanoparticles to form hybrid nanofluid flow in porous media over a Riga plate. The thermal and physical conditions, along with the nanofluid composition, significantly influence thermal propagation in applications such as filtration technologies, chemical reactors, and geothermal reservoirs. Through numerical methods, the study examines the impact of key physical factors, such as, electromagnetic force, medium permeability, quadratic radiation intensity, nanoparticle volume fraction, and the Casson fluid index—on the flow, and temperature distribution.

2. Model development and formulation of governing equations

The development of the governing equations for the flow and heat transfer phenomenon is done by taking cognizance of the following assumptions:

- The flow is steady, incompressible with the base fluid being a Casson fluid, with MoS_2 and SiO_2 nanoparticles uniformly suspended in H_2O.
- The flow occurs in a slip and convective boundary layer along a porous Riga plate. The velocity components in the x and y directions are u and v, with surface velocities given by $v_s(x) = v_0 e^{x/L}$ and $u_s(x) = U_0 e^{x/L}$. The plate's temperature is $\vartheta_s(x) = \vartheta_\infty + \vartheta_0 e^{2x/L}$.
- Convective heat transfer is characterized by $h_f = h\sqrt{U_0 e^{-x/2L}/2L}$. The hybrid nanofluid is electrically conducting, with the Lorentz force acting perpendicular to the plate.
- The plate consists of permanent magnets and electrodes, generating an electromagnetic field.
- A single-phase hybrid nanofluid model is used, and the rheological behavior is governed by the Cauchy stress tensor.
- The flow is influenced by an externally applied Lorentz force, and the porous structure of the Riga plate is modeled using the Darcy-Brinkman formulation to account for flow resistance.

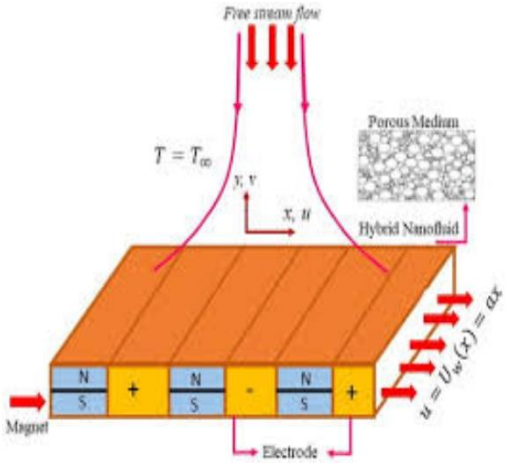

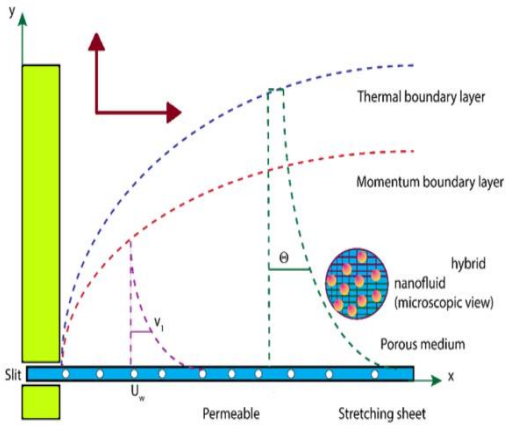

Figure 1: Sketch of the Riga plate
Figure 2: Flow Configuration and coordinate system

Incorporating the highlighted assumptions and using the boundary layer approximations, the governing equations are derived and expressed as follows:

$$\frac{\partial u}{\partial x}+\frac{\partial v}{\partial y}=0, \tag{1}$$

$$\rho_{hf}\left(u\frac{\partial u}{\partial x}+v\frac{\partial u}{\partial y}\right)=\mu\left(1+\frac{1}{\gamma}\right)\frac{\partial^2 u}{\partial y^2}-\left(1+\frac{1}{\gamma}\right)\frac{\mu_{hf}}{K_p}+\frac{H_0 J_0 \pi}{8}\exp\left(-\frac{\pi}{c}ye^{x/2L}\right), \tag{2}$$

$$(\rho Cp)hf\left(u\frac{\partial T}{\partial x}+v\frac{\partial T}{\partial y}\right)=\frac{\partial}{\partial y}\left(khf(T)\frac{\partial T}{\partial y}\right)-\frac{\partial qr}{\partial y}+\mu_{hf}\left(1+\frac{1}{\gamma}\right)\left(\frac{\partial u}{\partial y}\right)^2-Q_0(T-T_\infty), \tag{3}$$

The relevant boundary conditions for the governing equations (1-3) are defined as:

$$u=u_w(x)\alpha+g\frac{\mu_{hf}}{\rho_{hf}}\frac{\partial u}{\partial y}, v=v_w,\ -k_{hf}(T)\frac{\partial T}{\partial y}=h_f(T_w-T) \text{ at } y=0,$$
$$u\to 0, T\to T_\infty, \text{ as } y\to\infty. \tag{4}$$

The continuity equation is expressed in equation (1), while the flow momentum and thermal energy equations are represented by equations (2) and (3), respectively. On the RHS of equations (2) and (3) are the convective derivatives, capturing the transport of momentum and energy due to fluid motion. In these models:

- u and v denote the velocity components in the x and y-directions, T represents temperature.
- μ_{hf} is the dynamic viscosity of the hybrid nanofluid, γ is the Casson parameter characterizing the non-Newtonian nature of the base fluid, K defines the porosity of the medium.
- ρ_{hf} is the density of the hybrid nanofluid, $(\rho C_p)_{hf}$ indicates the

specific heat capacity of the hybrid nanofluid.
- k_{hf} is the thermal conductivity of the hybrid nanofluid.

The Lorentz force acting on the fluid is modeled by $\bar{F} = \bar{J} \times \bar{B} = \frac{H_0 J_0 \pi}{8\rho_{hf}} \exp\left(-\frac{\pi}{c} y\right)$, which characterizes the electromagnetic force induced by the Riga plate. Here:
J_0 defines the surface current density from the electrodes,
M_0 reflects the magnetization of the Riga plate,
c stands for the characteristic width of the magnets/electrodes,
α denotes the stretching or contracting rate of the surface,
$g = Ae^{x/2L}$ connotes the variable slip velocity at the boundary.

Lastly, the term $\frac{\partial q}{\partial y}$ in equation (3) models the radiative heat flux, which is described using the Rosseland approximation.

$$qr = -\frac{4}{3k_r}\nabla(e_r), \tag{5}$$

where $e_r = \sigma_r \vartheta^4$ is the power emission black body, σ_r indicate Stefan-Boltzmann, and k_r present mean absorption individually. Applying Taylor's series, T is express in terms of T_∞ as

$$T^4 = T_\infty^4 + 4(T - T_\infty)T_\infty^3 + 6(T - T_\infty)^2 T_\infty^2 + 4(T - T_\infty)^3 T_\infty + \ldots \tag{6}$$

The simplified form of equation (7) when neglecting quadratic term and other high terms becomes

$$T_\infty^4 \approx 3TT_\infty^4 - 8TT_\infty^3 + 16TT^2T_\infty^2, \tag{7}$$

introducing the Rosseland approximation into equation (8), the flow thermal quadratic radiation is obtained in relation to Thriveni and Mahanthesh [17]

$$q_r = -\frac{4\sigma_r}{k_r}\frac{\partial T^4}{\partial y} = -\frac{4\sigma_r}{k_r}\frac{\partial}{\partial y}(T^4 \approx 3T_\infty^4 - 8TT_\infty^3 + 6T^2T_\infty^2) = \frac{32\sigma_r T_\infty^3}{3k_r}\frac{\partial T}{\partial y} - \frac{24\sigma_r T_\infty^2}{3k_r}\frac{\partial}{\partial y}(T^2), \tag{8}$$

Therefore, from equation (8), the nonlinear radiation term is simplified as:

$$\frac{\partial qr}{\partial y} = \frac{32\sigma_r T_\infty^3}{3k_r}\frac{\partial^2 T}{\partial y^2} - \frac{24\sigma_r T_\infty^2}{3k_r}\frac{\partial^2 (T^2)}{\partial y^2}. \tag{9}$$

The energy equation (3) is thus modified by incorporating equation (9). Additionally, the governing equations (1-4) are transformed into ordinary form using the following similarity variables and stream function η:

$$\eta = y\sqrt{\frac{u_0}{2Lv_f}}e^{x/2L}, u = \frac{\partial \eta}{\partial y} = u_0 e^{x/L}u'(\eta), v = -\frac{\partial \eta}{\partial y} = -\sqrt{\frac{v_f u_0}{2L}}e^{x/2L}(u(\eta) + \eta u'(\eta)), \tag{10}$$

$$\xi = \sqrt{2Lvu_0}e^{x/2L}u(\eta), T = (\phi_s - T_\infty)\phi(\eta) + T_\infty.$$

The linear temperature-dependent thermal conductivity in equation (3) is expressed as:

$$k_{hf}(T) = k_{hf}\left(1 + \epsilon\frac{T - T_\infty}{T_w - T_\infty}\right) = k_{hf}(1 + \epsilon\phi). \tag{11}$$

Where ϵ describes the variable thermic conductivity. By incorporating equation (9) in the governing equations, a set of ordinary differential equations listed below is obtained:

$$\frac{\mu_{hf}}{\mu_f}\frac{\rho_f}{\rho_{hf}}\left(1 + \frac{1}{\gamma}\right)u''' + uu'' - 2u'^2 + \beta\frac{\rho_f}{\rho_{hf}}\exp(-m\eta) - \frac{\mu_{hf}}{\mu_f}\frac{\rho_f}{\rho_{hf}}\left(1 + \frac{1}{\gamma}\right)Pu' = 0, \tag{12}$$

$$\frac{k_{hf}}{k_f}[(1+\epsilon\phi)\phi'' + \epsilon\phi'^2] + \frac{(\rho Cp)_{hf}}{(\rho Cp)_f} Pr(u\phi' - 2u'\phi) + \frac{\mu_{hf}}{\mu_f}\left(1+\frac{1}{\gamma}\right) PrEcu''^2 - PrQ\phi - 2R\phi'' - 3R[(\phi_r - 1)\phi'^2 + (1+(\phi_r-1)\phi)\phi''] = 0. \quad (13)$$

The transformed wall conditions are:

$$u'(0) = \alpha + \delta\frac{\mu_{hf}}{\mu_f}\frac{\rho_f}{\rho_{hf}}u''(0), u(0) = S, \phi'(0)(1+\epsilon\phi(0)) = -\frac{k_f}{k_{hf}}Bi(1-\phi(0)), \quad (14)$$

$u'(\eta) \to 0, \phi(\eta) \to 0$, as $\eta \to \infty$.

The embedded parameters are describes as follows: u and ϕ are respectively the transformed fluid velocity and temperature, $m = \frac{\pi}{c}\sqrt{\frac{2L\nu_f}{W_0}}$ defines electrodes and magnets width variable, $\beta = \frac{LH_0J_0\pi}{4W_0^2\rho_f}a$ is the modified Hartmann number, $Bi = \frac{h}{k_f}\sqrt{\nu_f}$ is the Biot number, $Pr = \frac{(\mu Cp)_f}{k_f}$ is Prandtl number, $S = -\frac{v_0}{\sqrt{\frac{W_0\nu_f}{2L}}}$ represents the wall porosity, $Ec = \frac{w_s^2}{Cp(\vartheta_s - \vartheta_\infty)}$ represents Eckert number, $R = \frac{16\sigma_r\vartheta_\infty^3}{3k_fk_r}$ represents radiation, $\delta = g\frac{\mu_f}{\rho_f}\sqrt{\frac{W_0}{2L\nu_f}}$ describes variable velocity slip, $\phi_r = \frac{\vartheta_s}{\vartheta_\infty}$ showcases the thermal ratio, $Q = \frac{Q_0L^2}{(\mu Cp)_f}$ symbolizes the heat loss, $P = \frac{L^2}{K}$ connotes medium porosity respectively. The nanofluid and the hybrid nanofluid thermophysical quantities are listed as:

$\frac{\mu_{nf}}{\mu_f} = \frac{1}{(1-\psi_a)^{2.5}}$ and $\frac{\mu_{hf}}{\mu_f} = \frac{1}{(1-\psi_a)^{2.5}(1-\psi_b)^{2.5}}$ define dynamic viscosity,

$\frac{(\rho Cp)_{nf}}{(\rho Cp)_f} = (1-\psi_a) + \psi_a\frac{(\rho Cp)_{a1}}{(\rho Cp)_f}$, $\frac{(\rho Cp)_{hf}}{(\rho Cp)_{nf}} = (1-\psi_b) + \psi_b\frac{(\rho Cp)_{b1}}{(\rho Cp)_{nf}}$,and

$\frac{(\rho Cp)_{hf}}{(\rho Cp)_f} = (1-\psi_b)\left[(1-\psi_a) + \psi_a\frac{(\rho Cp)_{a1}}{(\rho Cp)_f}\right] + \psi_b\frac{(\rho Cp)_{b1}}{(\rho Cp)_f}$ define thermal capacity,

$\frac{\rho_{nf}}{\rho_f} = (1-\psi_a) + \psi_a\frac{\rho_{a1}}{\rho_f}$ and $\frac{\rho_{hf}}{\rho_f} = (1-\psi_b)\left[(1\psi_a) + \psi_a\frac{\rho_{a1}}{\rho_f}\right] + \psi_b\frac{\rho_{b1}}{\rho_f}$ define density,

$\frac{k_{nf}}{k_f} = \frac{2k_f + k_{s1} - 2\psi_a(k_f - k_{s1})}{2k_f + k_{s1} + \psi_a(k_f - k_{s1})}$, $\frac{k_{hf}}{k_{nf}} = \frac{2k_{nf} + k_{s2} - 2\psi_b(k_{nf} - k_{s2})}{2k_{nf} + k_{s2} + \psi_b(k_{nf} - k_{s2})}$, and

$\frac{k_{hf}}{k_f} = \frac{k_{hf}}{k_{nf}} \times \frac{k_{nf}}{k_f}$ define heat conductivity.

2.1. Quantities of Technological usefulness

The benefits of engineering community are quantified in the skin friction coefficient, and heat transfer phenomenon (the Nusselt number). These two quantities are expressed as:

$$Cf_x = \frac{\tau_s}{\rho_f w_s^2}, Nu_x = \frac{q_s e^{x/2L}}{k_f(\vartheta_s - \vartheta_\infty)}, \quad (15)$$

with τ_w and q_w being the shear stress and thermal flux at the boundary respectively.

$$\tau_w = \mu_{hf}\left(1+\frac{1}{\gamma}\right)\partial u_y\Big|_{y=0}, q_s = -k_{hf}(\vartheta)\partial\vartheta_y + \partial q_y\big|_{y=0}. \quad (16)$$

Using equations (10) and (11) on the combined equations of (15) and (16), resulting dimensionless equations are:

$$2(Re_x)^{1/2}Le^{-x/2L}Sf = \frac{\mu_{hf}}{\mu_f}\left(1+\frac{1}{\gamma}\right)u''(0), \tag{17}$$

$$Tf(Re_x)^{-1/2} = -\left[\frac{k_{hf}}{k_f}(1+\epsilon\phi(0)) + 3R(1+(\phi_r-1))\phi(0) - 2R\right]\phi'(0). \tag{18}$$

The base fluid and the thermophysical properties are tabulated in Table 1

Table 1: The nanoparticles and its thermophysical properties

Thermofluids	$C_p(J/kgK)$	$\rho(kg/m^3)$	$k(W/mK)$	$\sigma(\Omega/m)^{-1}$	Pr
SiO_2	730.00	2650.00	1.5	2.09×10^4	-
MoS_2	397.746	5060.00	43.5	6.30×10^7	-
H_2O	4179.00	997.10	0.61300	0.5×10^{-6}	6.2

3. Results and Discussion

The governing equations (12-14) are solved numerically using the bvp4c solver in MATLAB software. This bvp4c is appropriate solving coupled nonlinear ordinary differential equations for boundary layer flow problems. It is capable of solving highly nonlinear and coupled systems of differential equations usually found in fluid dynamics. It is ideal for problems where conditions are specified at multiple locations and famous for its stability and accuracy for highly nonlinear differential equations. Thus, the boundary value problem (12-14) is numerically solved and the result is validated with existing results in the literature under limiting conditions of $Pr = 0.7,\ S = 3.0,\ P = Q = z = Ec = \delta = Nr = \epsilon = 0$ and $Bi \to \infty$. The results agree excellent with existing related studies as depicted in Table 2.

Table 2: Computational values of $u''(0)$ and $-\phi'(0)$ in the absence of volume fraction for $\lambda = -1$

	$u''(0)$		$-\phi'(0)$	
Authors	**First Solution**	**Second Solution**	**First Solution**	**Second Solution**
Wahid et al. [25]	2.390814	-0.9722247	1.771237	0.848316

Sarka et al. [26]	2.3908136	-0.9721280	1.7712383	0.8478486
Current	2.390813634	-0.972128864	1.771237307	0.847748274

3.1. Graphical Results

For better understanding of the involved parameters, figures 3-10 are sketched for variations in the flow dynamical terms.

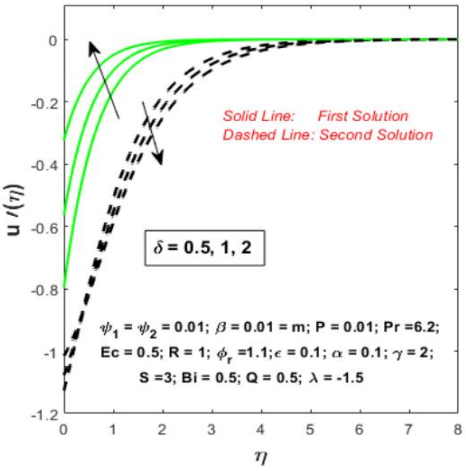

Figure 3: Trend of velocity field for growth in δ

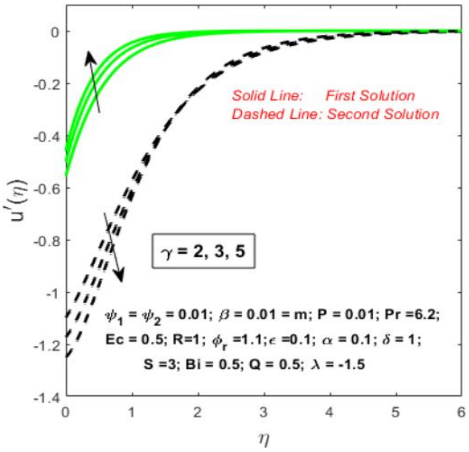

Figure 4: Velocity trend for rising γ

Figure 3 illustrates the effect of the velocity slip parameter δ on the velocity profiles for both the first and second solutions. Dual solutions, typical in nonlinear boundary layer flows, emerge clearly. For the first solution, a rise in δ enhances the Casson hybrid nanofluid velocity, attributed to reduced wall friction, which facilitates momentum transfer and raises fluid motion. In contrast, the second solution fosters a decline in velocity with rising δ. Figure 4 presents the influence of the Casson fluid parameter γ on the hybrid nanofluid velocity profiles. In the first solution, increasing γ enhances fluid velocity due to a reduction in yield stress, causing the fluid to behave more Newtonian and flow more freely—indicating a stable branch. In contrast, the second solution, representing an unstable branch, shows decreasing velocity with higher γ, as stronger non-Newtonian effects increase effective viscosity and slow the flow.

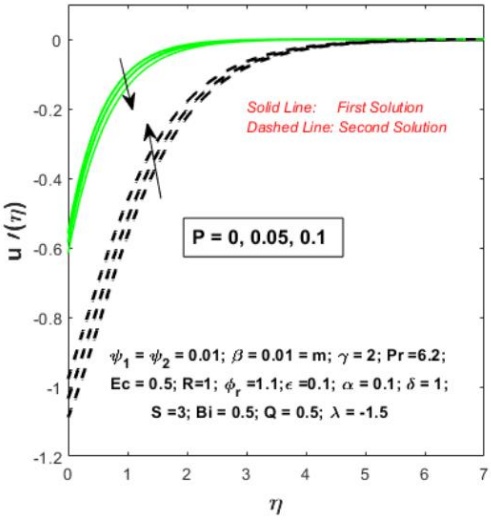

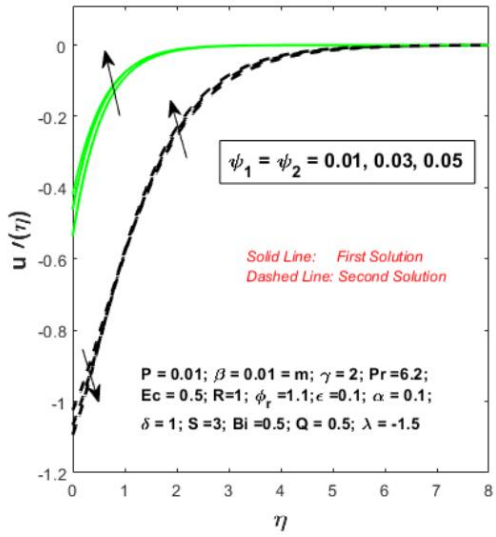

Figure 5: Velocity distribution for rising P **Figure 6**: Velocity profiles for variation in ψ

Figure 5 displays the influence of the porosity parameter P on the velocity profiles of the hybrid Casson nanofluid. In the first solution, increasing P intensifies the resistance due to reduced permeability, leading to a thinner momentum boundary layer and slower flow. Conversely, the second solution exhibits an expanded boundary layer as P rises, reflecting enhanced medium permeability and increased fluid velocity—demonstrating a delicate balance between flow resistance and permeability. Figure 6 shows the effect of the modified Hartmann number ψ on the velocity field. A growth in ψ thickens the hydrodynamic boundary layer and accelerates fluid motion in both solution branches, driven by the augmented electromagnetic force overcoming viscous resistance.

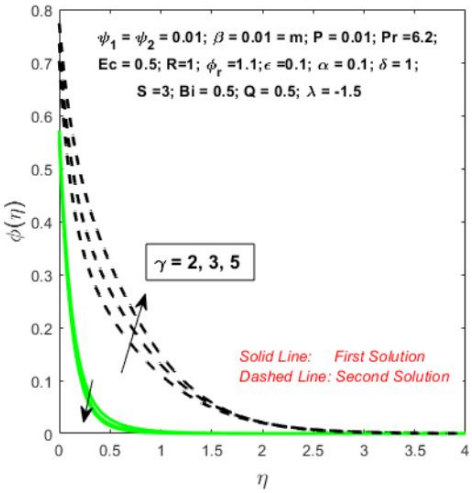

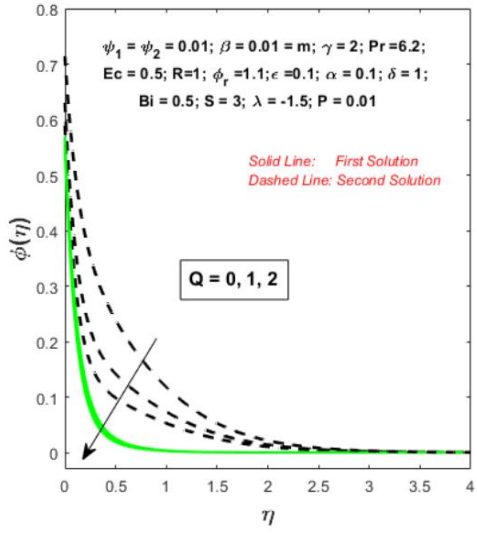

Figure 7: Temperature profiles for variation in γ **Figure 8:** Thermal field for varying Q

Figure 7-10 portray the thermal behaviour of some selected parameters as other terms are fixed. Figure 7 examines the influence of the Casson parameter γ on the thermal distribution of the hybrid Casson nanofluid. In the second solution branch, increasing γ amplifies the thermal profile. This is because higher γ intensifies the shear-thinning behaviour, reducing the yield stress and resulting in steeper velocity gradients near the wall. These gradients, in turn, generate more viscous dissipation, which elevates the fluid temperature

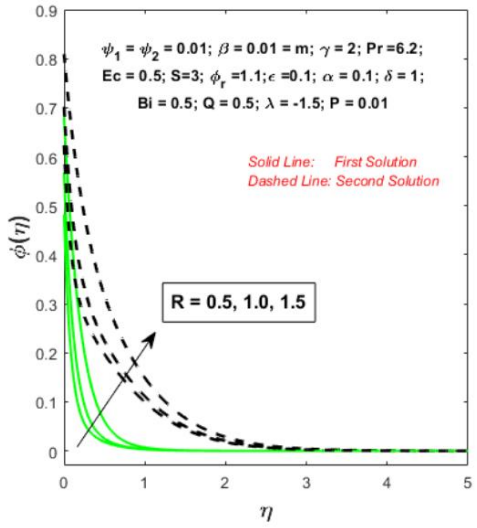

Figure 9: Thermal profile for different R

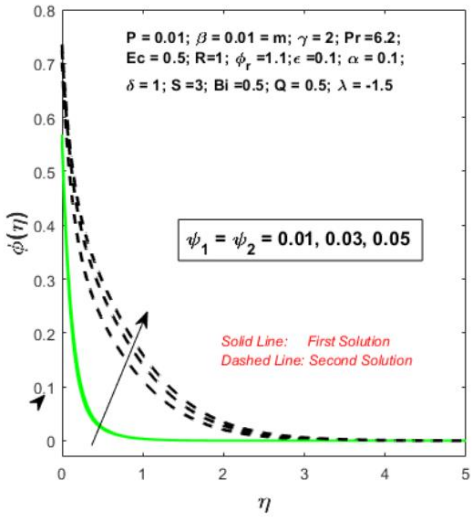

Figure 10: Impact of ψ on heat propagation

. Conversely, in the first solution, a rise in γ slightly suppresses the thermal distribution. This occurs due to smoother velocity transitions and reduced local fluid resistance, which diminish internal heat generation. Figure 8 highlights the role of the heat loss parameter Q. As Q increases, the temperature profile significantly decreases, and the thermal boundary layer becomes thinner. Physically, this parameter represents energy loss to the surroundings. A higher Q leads to stronger thermal dissipation, reducing the heat retained within the system, which is evident in the steep decline in temperature near the boundary surface.

Figure 9 depicts the effect of the thermal radiation parameter R. As R increases, the temperature distribution improves markedly. This is because radiation promotes energy transport via electromagnetic wave interactions, boosting the internal energy of the nanofluid. As a result, more heat is absorbed and retained within the flow domain, leading to a thicker thermal boundary layer and elevated temperature profiles. Figure 10 explores the impact of ψ, the nanoparticle volume fraction parameter, on the thermal field. An increase in ψ leads to a broader thermal boundary layer and higher surface temperatures. The inclusion of $MoS_2 - SiO_2$ nanoparticles enhance the thermal conductivity and specific heat capacity of the base Casson fluid. These suspended particles improve the fluid's ability to store and conduct heat, which results in

improved thermal performance. The enhanced heat storage is particularly beneficial in systems requiring effective energy retention and controlled heat propagation, such as solar collectors and thermal filtration technologies.

4. Conclusion

This study investigated the flow dynamics and thermal efficiency of a water-based Casson MoS_2-SiO_2/H_2O hybrid nanofluid under the influence of quadratic thermal radiation, slip effects, and quadratic nanofluid radiative heat absorption in porous media with heat loss over a Riga plate. The theoretical model, characterized by nonlinear equations and variable thermal conductivity, was solved using a numerical method. The findings are significant for advancing thermal systems, including industrial heat exchangers, electronic cooling devices, and solar energy collectors. The study highlights the potential for thermal performance using Casson-based hybrid nanofluids in permeable media, paving the way for energy-efficient next-generation technologies. The key insights from this investigation include:

- The fluid flow and heat transfer rates are influenced by the porous medium, which contributes to enhanced heat exchange dynamics.
- The rheological properties of the Casson fluid affected the flow dynamics of the suspended MoS_2 and SiO_2 nanoparticles.
- The electromagnetic properties of the Riga plate optimized thermal propagation mechanisms, enhancing nanoparticle dispersion and boundary layer dynamics.
- Convective heat loss was effectively reduced through maximized nanoparticle loading and radiation effects, highlighting the synergy between convective cooling and radiative heat transfer for improved system performance.

References

[1] Behera, U. S., Sangwai, J. S., & Byun, H. S. (2025). A comprehensive review on the recent advances in applications of nanofluids for effective utilization of renewable energy. *Renewable and Sustainable Energy Reviews*, 207, 114901.

[2] Mahian, O., Bellos, E., Markides, C. N., Taylor, R. A., Alagumalai, A., Yang, L., ... & Wongwises, S. (2021). Recent advances in using nanofluids in renewable energy systems and the environmental implications of their uptake. *Nano Energy*, 86, 106069.

[3] Yıldızay, H. D., Bekmezci, M., & Şen, F. (2025). Nanofluids and engineering applications: A review. *Journal of Scientific Reports-A*, (060), 126-149.

[4] S.U.S. Choi, J.A. Eastman, Enhancing thermal conductivity of fluids with nanoparticles, *ASME Int. Mech. Engin. Congress and Exposition*, 11 (1995) 12-17.

[5] J. Buongiorno, Convective transport in nanofluids, *J. Heat Transfer*, 128(3) (2005) 240-250.

[6] Fatunmbi, E. O., Ramonu, O. J., & Salawu, S. O. (2023). Analysis of heat transfer phenomenon in hydromagnetic

micropolar nanoliquid over a vertical stretching material featuring convective and isothermal heating conditions. *Waves in Random and Complex Media*, 1-20.

[7] Salawu, S. O., Fatunmbi, E. O., & Okoya, S. S. (2021). MHD heat and mass transport of Maxwell Arrhenius kinetic nanofluid flow over stretching surface with nonlinear variable properties. *Results in Chemistry*, 3, 100125.

[8] M. Ferdows, MD. Shamshuddin, S.O. Salawu, Shuyu Sun, Thermal cooling performance of convective non-Newtonian nanofluid flowing with variant power-index across moving extending surface, *Scientific Reports*, 12(1) (2022) 8714.

[9] Weirong Xiu, S.O. Salawu, O.Y. Oludoun, O.M. Ogunlaran, A.B. Disu, Combined impact of Lorentz force, micro-rotation, and thermomigration of particles: Dynamics of micropolar fluids experiencing nonlinear thermal radiation and activation energy, *J. of Magnetism and Magnetic Materials*, 569 (2023) 170447.

[10] Suneetha, S., Subbarayudu, K., & Reddy, P. B. A. (2022). Hybrid nanofluids development and benefits: A comprehensive review. *Journal of Thermal Engineering*, 8(3), 445-455.

[11] Alanazi, M. M., Hendi, A. A., Raza, Q., Rehman, M. A., Qureshi, M. Z. A., Ali, B., & Shah, N. A. (2023). Numerical computation of hybrid morphologies of nanoparticles on the dynamic of nanofluid: The case of blood-based fluid. *Axioms*, 12(2), 163.

[12] Nabil, M. F., Azmi, W. H., Hamid, K. A., Zawawi, N. N. M., Priyandoko, G., & Mamat, R. (2017). Thermo-physical properties of hybrid nanofluids and hybrid nano lubricants: a comprehensive review on performance. *International Communications in Heat and Mass Transfer*, 83, 30-39.

[13] Fatunmbi, E. O., Adeosun, A. T., & Salawu, S. O. (2023). Dynamics of melting heat transfer of a micropolar nanofluid over an electromagnetic actuator with irregular thickness and non-uniform heat source. *International Journal of Applied and Computational Mathematics*, 9(3), 45.

[14] Salawu, S. O., Yusuf, T. A., Fatunmbi, E. O., & Obalalu, A. M. (2024). Dynamics of tri-hybridized Prandtl-Eyring thermal water-based magneto-nanofuids flow over double stretched wedge sheets experiencing force convection. *Forces in Mechanics*, 15, 100270.

[15] Fatunmbi, E. O., Mabood, F., Salawu, S. O., Obalalu, M. A., & Sarris, I. E. (2024). Exploration of melting heat transfer and entropy generation in a magnetized hybrid nanoliquid over an extending sheet of varying thickness. *Partial Differential Equations in Applied Mathematics*, 11, 100835.

[16] Fatunmbi, E. O., & Okoya, S. S. (2021, June). Quadratic mixed convection stagnation-point flow in hydromagnetic Casson

nanofluid over a nonlinear stretching sheet with variable thermal conductivity. In *Defect and diffusion forum* (Vol. 409, pp. 95-109). Trans Tech Publications Ltd.

[17] Salawu, S. O., Yusuf, T. A., Fatunmbi, E. O., & Obalalu, A. M. (2024). Dynamics of tri-hybridized Prandtl-Eyring thermal water-based magneto-nanofuids flow over double stretched wedge sheets experiencing force convection. *Forces in Mechanics*, 15, 100270.

[18] Gbadeyan, J. A., Titiloye, E. O., & Adeosun, A. T. (2020). Effect of variable thermal conductivity and viscosity on Casson nanofluid flow with convective heating and velocity slip. *Heliyon*, 6(1).

[19] Souayeh, B., Reddy, M. G., Sreenivasulu, P., Poornima, T. M. I. M., Rahimi-Gorji, M., & Alarifi, I. M. (2019). Comparative analysis on non-linear radiative heat transfer on MHD Casson nanofluid past a thin needle. *Journal of Molecular Liquids*, 284, 163-174.

[20] Wang, F., Asjad, M. I., Zahid, M., Iqbal, A., Ahmad, H., & Alsulami, M. D. (2021). Unsteady thermal transport flow of Casson nanofluids with generalized Mittag–Leffler kernel of Prabhakar's type. *Journal of Materials Research and Technology*, 14, 1292-1300.

[21] Hayat, T., Abbas, T., Ayub, M., Farooq, M., & Alsaedi, A. (2016). Flow of nanofluid due to convectively heated Riga plate with variable thickness. *Journal of Molecular Liquids*, 222, 854-862.

[22] Rizwana, R., & Nadeem, S. (2020). Series solution of unsteady MHD oblique stagnation point flow of copper-water nanofluid flow towards Riga plate. *Heliyon*, 6(10).

[23] Fatunmbi, E. O., & Adeosun, A. T. (2020). Nonlinear radiative Eyring-Powell nanofluid flow along a vertical Riga plate with exponential varying viscosity and chemical reaction. *International Communications in Heat and Mass Transfer*, 119, 104913.

[24] Fatunmbi, E. O., Oke, A. S., & Salawu, S. O. (2023). Magnetohydrodynamic micropolar nanofluid flow over a vertically elongating sheet containing gyrotactic microorganisms with temperature-dependent viscosity. *Results in Materials*, 19, 100453.

[25] N.S. Wahid, N.M. Arifin, N.S. Khashi, I. Pop, N. Bachok, M.E.H. Hafidzuddin, Hybrid nanofluid stagnation point flow past a slip shrinking Riga plate, *Chinese Journal of Physics*, 78 (2022) 180–193.

[26] A. Sarkar, Go. Mandal, D. Pal, Heat transfer inspection and entropy optimization in water/$MoS_2 - SiO_2$ Casson hybrid nanofluid flow with quadratic radiation ray over an exponentially contracting permeable Riga surface: Duality and stability analysis, *Thermal*.